Available online at www.sciencedirect.com
ScienceDirect
Procedia Engineering 136 (2016) 216 – 219
Procedia Engineering
www.elsevier.com/locate/procedia

The 20th International Conference: Machine Modeling and Simulations, MMS 2015

Thermal-stress analysis of beam loaded by 3 point bending

Milan Sapieta[a,*], Vladimír Dekýš[a], Alžbeta Sapietová[a]

[a]*University of Žilina, Faculty of Mechanical Engineering, Department of Applied Mechanics, Univerzitná 1, 010 26 Žilina, Slovakia*

Abstract

This paper describes investigation of experimental thermal stress analysis of stainless steel which was loaded by three-point bending. Loading took place cyclically with constant amplitude. The measurements were performed using as contactless scanning of infrared radiation emitted during loading from the face of specimen. The results were evaluated according to the theory of thermoelasticity. After evaluation of the results we get stress distribution of first invariant on the front face of the specimen.

Peer-review under responsibility of the organizing committee of MMS 2015

Keywords: thermal; 3 point bending; stress; mechanical load, experimental measurement

1. Introduction

In recent years, infrared thermography developed from rarely used method of the method with an increasing popularity among users. Examples of dynamic thermography are Thermoelastic Stress analysis (TSA), pulse thermography and lock-in thermography. Combining of infrared detectors and thermal sensors with advanced signal processing creates a practical tool for studying thermal-stress characteristics of the materials and constructions.

Thermoelastic Stress analysis is used by engineers and scientists for more than 50 years to solve practical problems. It works on the principle of recording energy released during loading in the elastic range. When the load is removed, the body returns to its original position (elasticity) and its initial temperature (thermoelasticity).

* Corresponding author. Tel.: + 421 41 513 2965.
E-mail address: milan.sapieta@fstroj.uniza.sk

Peer-review under responsibility of the organizing committee of MMS 2015
doi:10.1016/j.proeng.2016.01.200

2. Thermoelastic stress analysis

Thermoelastic Stress analysis is a non-contact experimental method based on the measurement of infrared radiation which is emitted from the surface of the component dynamically linear elastic deformation loaded. Kelvin was the first who engaged in the thermoelastic effect and the basic equations to describe the thermoelastic effect were formulated by Darken and Curry [1–4]. The general form of the heat transfer for flexible body is derived from the energy equation and can be written in the form:

$$\rho c_\varepsilon \frac{dT}{dt} - \frac{\partial}{\partial x_j}\left(k\frac{\partial T}{\partial x_j}\right) = \rho r + \sigma_{ij}\frac{\partial \varepsilon_{ij}}{\partial t} - \rho\frac{\partial \Psi}{\partial V_k}\frac{dV_k}{dt} + \rho T\frac{\partial^2 \Psi}{\partial T \partial V_k}\frac{dV_k}{dt} \quad (1)$$

In Eq. 1 was used Einstein notation, where ρ is the density, c_ε the specific heat capacity at constant deformation, T is the absolute temperature, k is the thermal conductivity tensor, σ_{ij} and ε_{ij} are the stress and deformation tensors, r is the internal heat source per unit volume and Ψ is the Helmholtz free energy, which is dependent on k independent of the internal state variables V_k [5]. Provided that the elastic material properties and constant material coefficients are temperature independent, may be derived three-dimensional heat equation:

$$\rho C_\varepsilon \dot{T} - k\Delta^2 T = T_0\left(-\frac{E\alpha}{1-2\upsilon}\right)\dot{\varepsilon}_I^e + \alpha_p \sigma_{ij}\dot{\varepsilon}_{ij}^p \quad (2)$$

The equation for heat conduction will include the creation of the thermoelastic and the thermoplastic heat. Parameter $\varepsilon_\mathrm{I}^\mathrm{e}$ denotes the first invariant of elastic deformation tensor, ε_{ij}^p is the plastic part of the deformation tensor, α is the coefficient of thermal expansion, E is Young's modulus, υ is Poisson's ratio and T_0 is the initial temperature [6–8]. Non-dimensional coefficient α_p is the ratio of the total plastic work to plastic work, which is converted to heat. The value $\alpha_p \cong 1$ because of only a small part of the plastic work (obtained energy at cold forming) is used to change the inner properties of the material [9–13]. Therefor the thermoplastic area will be neglected and relationship will be formulated only for thermo-elastic area, which has the following form:

$$\Delta T = \frac{\alpha T_0}{\rho c_p}\Delta\sigma_{ii} \quad (3)$$

where c_p is the specific heat capacity under constant pressure and its relationship with c_ε is as follows:

$$c_\varepsilon = c_p - \frac{2E\alpha^2 T}{\rho(1-\upsilon)} \quad (4)$$

3. Measurement

For this experiment was selected beam specimen with a length of 50 mm and square cross-section with a width of side 10 mm. Material of specimen was selected stainless steel AISI 304. To the surface of the sample was applied emission spray. This spray is primarily specified for long-wave IR cameras but for homogenizing the specimen surface is currently shown to be the best possible solution. To eliminate the influence of external factors during the measurement specimen was placed between polystyrene plates of thickness 80 mm. Polystyrene plates were placed from 3 sides.

The specimen was cyclic loaded on a test load machine with three-point bending. Loading frequency was 105 Hz and frame rate 383 Hz was chosen because of achieving the maximum possible resolution of IR camera. According to the theory it is recommended to carry out at least 4 images for one of the loading period. Thus, this measurement was slightly under-sampled but ultimately on the quality of the results it hasn't had any effect. The specimen was loaded cyclically only to pressure so that by the static load force, this force will be called static component of the load force in the next section, then was chosen dynamic load component which was periodically changed. The dynamic component was always chosen so as to be lower than the static component because of the specimen was not loaded with the tensile and there was no risk the loss of stability. There were the 5 load cases chosen for beam specimen, Table 1.

Table 1. Load cases of beam specimen.

Measurement	1.	2.	3.	4.	5.
The static component of the loading force (kN)	1	2	3	4	5
The dynamic component of the loading force (kN)	0.5	1	2	3	4

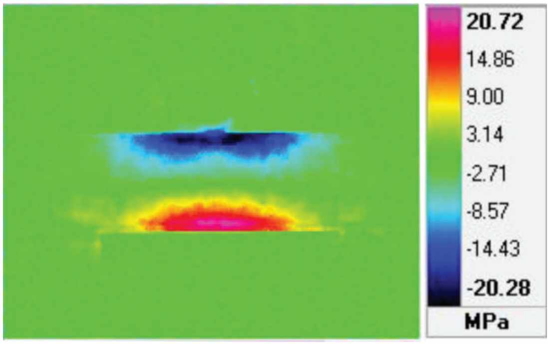

Fig. 1. Principal stress distribution on beam of specimen for load of 0.5 kN.

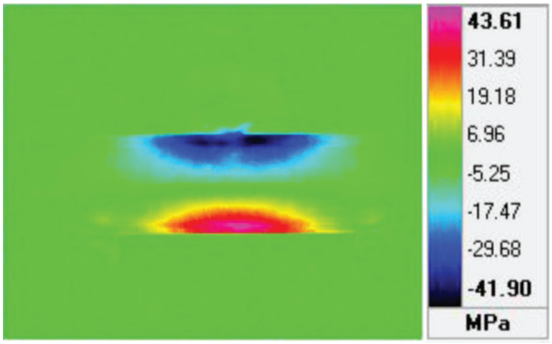

Fig. 2. Principal stress distribution on beam of specimen for load of 1 kN.

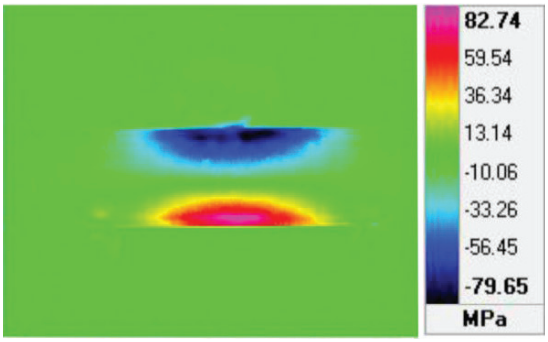

Fig. 3. Principal stress distribution on beam of specimen for load of 2 kN.

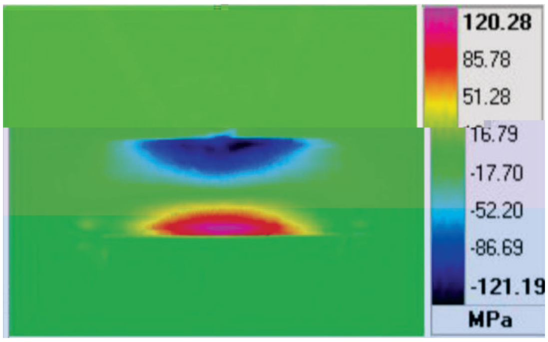

Fig. 4. Principal stress distribution on beam of specimen for load of 3 kN.

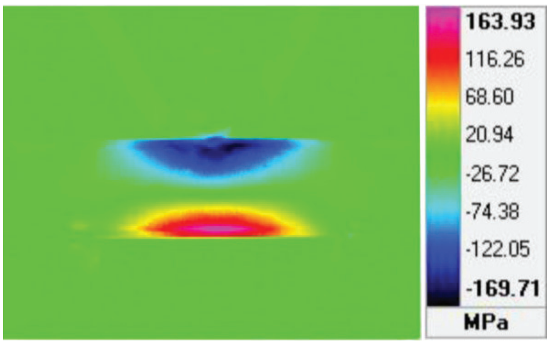

Fig. 5. Principal stress distribution on beam of specimen for load of 4 kN.

Substituting material properties for this type of material was achieved following distribution of stress fields (Fig. 1–4). With increasing value of load value of the sum of the principal stresses.is also increased. There is minimum of stress (negative) on the top of the specimen where is load finger paced. This area is illustrated by blue color which represents loading longitudinal fibers with pressure. The lower part of the specimen, the area between the brackets is shown in red, which represents the longitudinal stress fibers to tensile. The maximum stress value is in the lower part and it is plotted in purple and minimum stress is plotted on top by dark blue.

4. Conclusion

This measurement is already the second type of analysis of this kind our research where we have chosen different kinds of loading (three-point bending) as in the first case where the specimen was loaded with tensile. Very important factor was the preparation of specimen and environment before measurement. Recorded surface of the specimen was homogenized using emission spray. This method has proven to be successful from previous measurements. The stored specimen in loading machine was covered by polystyrene plates in order to prevent penetration of reflected radiation from the environment. The selected sampling frequency has also been shown to be sufficient even though it was a slightly under-sampling. This frequency was chosen mainly in order to achieve the maximum possible resolution on the specimen surface to achieve the greatest accuracy in evaluating the stress field. The results of the thermal stress analysis have been changed linearly depending on the load. At the maximum load was reached value 163.71 MPa at tensile of fibers on the bottom of specimen and value 163.93 MPa at pressure of fibers on the top side of specimen. At the case of minimum load (Fig. 1) it is possible observed a slight drop of first invariant of stress on the vertical axis going through the center of specimen. This phenomenon cannot be observed in other load cases.

Acknowledgement

This work was supported by the Slovak Research and Development Agency under the contract No. APVV-0736-12.

References

[1] V. Vavilov, Thermal / Infrared testing, in: Nondestructive testing, Publishing house Spektr, Moscow, 2009.
[2] C.S. Welch, M.J. Zickel, Thermal coating characterization using thermoelasticity, in: D.O. Thomson, D.E. Chimenti, (Eds.), Review of Progress in Quantitative ondestructive Evaluation, vol. 12, Planum Press, NY, 1993.
[3] S.W Boyd, J.M. Dulieu-Barton, L. Rumsey, Stress analysis of finger joints in pultruded GRP materials, International Journal of Adhesion and Adhesives 26 (2006) 498–510.
[4] A. Chrysochoos, H. Louche, An infrared image processing to analyse the calorific affects accompanying strain localization, International journal of engineering science 38 (2001) 1759–1788.
[5] S. Desiderati, A. Salerno, Quantitative thermoelastic stress analysis in non adiabatic conditions, Proc. of SPIE 5405, 1987, 466–475.
[6] E.A. Pieczyska, S.P. Gadaj, W.K. Nowacki, Thermoelastic and thermoplastic effects during loading and unloading of austenitic steel, in: Quantitative infrared thermography 4, QIRT'98, Proceedings of Eurotherm Seminar No. 60, Lodz, Poland, 2000, pp. 112–116.
[7] J. Awrejcewicz, Y. Pyryev, Thermoelastic contact of a rotating shaft with a rigid bush in conditions of bush wear and stick-slip movements, International Journal of Engineering Science 40 (2002) 1113–1130.
[8] M. Sága, M. Vaško, P. Kopas, L. Jakubovičová, Identification of the hysteretic material model parameters and application on energy fatigue curve, Machine Dynamics Research, Warsaw University of Technology (2010) 79–87.
[9] A. Kaminski, J. Jouglar, M. Mergui, Y. Jourlin, A. Bouille, P.L. Vuillermoz, A. Laugier, Infrared Characterization of Hot Spots in Solar Cells with High Precision Due to Signal Treatment Processing, Solar Energy Mat. & Solar Cells 51 (1998) 233–242.
[10] M. Vasko, M. Saga, Solution of Mechanical Systems with Uncertainty Parameters using IFEA, Communications 11(2) (2009) 19–27.
[11] P. Kopas, M. Vasko, M. Handrik, Computational Modeling of the Microplasticization State in the Nodular Cast Iron, Applied Mechanics and Materials 474 (2014) 285–290.
[12] M. Saga, P. Kopas, M. Vasko, Some computational aspects of vehicle shell frames optimization subjected to fatigue life, Communications 12(4) (2010) 73–79.
[13] M. Zmindak, M. Saga, Structural Optimization of Trusss Structures for Deterministic and Nondeterministic Loads Using MATLAB, in: Proceedings of the VIIth International conference on numerical methods in continuum mechanics, High Tatras,1998, pp. 368–373.